

Cloning, expression, purification and crystallization of the N-domain from the α_2 subunit of the membrane-spanning Na,K-ATPase protein

Lisbeth Haue, Per A. Pedersen,
Peter L. Jorgensen and Kjell O.
Håkansson*

Biomembrane Center, August Krogh Institute,
Copenhagen University, Universitetsparken 13,
2100 Copenhagen OE, Denmark

Correspondence e-mail:
kohakansson@aki.ku.dk

The nucleotide-binding domain of the Na,K-ATPase ion pump was expressed with a His tag in *Escherichia coli* and purified. The soluble 24 kDa derivative consists of 214 amino-acid residues and was crystallized in the presence of NiCl₂. The crystals belong to space group *F*23, with unit-cell parameters $a = b = c = 147.5$ Å, and diffract to 3.1 Å. Complete data sets could be collected from native and thimerosal-treated crystals frozen in 50% sucrose. Five mercury positions were found and initial SIR phases calculated.

Received 13 March 2003
Accepted 16 April 2003

1. Introduction

Na,K-ATPase belongs to the P-type ATPase family and plays an important role in maintaining the plasma membrane potential in animal cells *via* ATP-fuelled sodium ion export (Skou, 1957) and potassium ion import. The structure of Na,K-ATPase has been extensively studied by electron crystallography (Deguchi *et al.*, 1977; Hebert *et al.*, 2001), but no atomic resolution structure is available. The direct agent of sodium and potassium ion transport, the α -subunit, is a multispan transmembrane (TM) helical protein with three soluble domains on the cytoplasmic side of the membrane. The P-domain, inserted between TM4 and TM5, contains an insertion called the N-domain, which binds ATP during the transport cycle. The crystallographic structure of the homologous sarcoplasmic reticulum Ca-ATPase (Toyoshima *et al.*, 2000; Toyoshima & Nomura, 2002) can be used to model large parts of the Na,K-ATPase molecule, but low sequence similarity and the presence of insertions and deletions in the N-domain prohibit homology modelling of this region. To address this question and at the same time to avoid the many problems associated with crystallization of membrane proteins, we cloned, expressed, purified and crystallized the cytoplasmic N-domain of the porcine α_2 isoenzyme.

2. Methods

A cloned full-length porcine α_2 Na,K-ATPase cDNA (P. A. Pedersen, unpublished work) was used as the template for PCR amplification. The N-domain sequence boundaries were estimated from the three-dimensional structure of Ca-ATPase and from alignment using *MultAlin* (<http://prodes.toulouse.inra.fr/>

multalin/multalin.html) and the Blossum 62 matrix (Toyoshima & Nomura, 2002; Corpet, 1988). The forward primer 5'-ACACACGAA-TTCATTAAGAGGAGAAATTAACATATGATGACCGTCGCCCATATG-3' and the reverse primer 5'-ACACACAAGCTTCTAT-TAGTGATGGTGATGGTGATGGTCAAT-CATGGACATGAGC-3' were designed to contain a Shine-Dalgarno ribosome-binding site and to encode a C-terminal sequence of six histidines. The PCR product was digested with *EcoRI* and *HindIII* and cloned into similarly digested pQE-40 (Qiagen), followed by transformation into XL-blue cells.

Cells were grown in 4 l of LB medium with 100 $\mu\text{g ml}^{-1}$ ampicillin in 1 l flasks and induced with 0.8 mM IPTG at an OD₆₀₀ of 0.4–0.6. After an additional 3 h of growth, the cells were harvested by centrifugation, washed with 50 mM Tris, 50 mM NaCl and stored at 253 K. Cells were thawed and sonicated in 10 ml of the same buffer and pellets were removed by centrifugation at 38 000g for 15 min. The supernatant was loaded onto a Ni-agarose column (5 ml; Qiagen) and washed with 50 mM Tris, 50 mM NaCl, 20 mM imidazole and 1 mM mercaptoethanol. The protein eluted approximately midway in an imidazole gradient from 20 mM to 0.5 M. Fractions containing the recombinant protein (7 ml) were immediately pooled and diluted with water to a volume of 50 ml and loaded onto a Q-Sepharose column (25 ml; Amersham Biotech) equilibrated with 50 mM Tris pH 7.5, 1 mM DTT. The protein was eluted with a 1 M/60 ml NaCl gradient. Fractions containing the α_2 Na,K-ATPase N-domain protein were stored frozen. The fractions were concentrated and diluted repeatedly with 10 mM Tris pH 7.5 in a Centricon YM-10 centrifugal filter (Millipore) and finally concentrated to 15 mg ml⁻¹ (estimated from a calculated ϵ_{280} of 0.52 ml mg⁻¹).

DTT (0.2 mM) was included in some preparations only, since it can reduce some of the metal ions used in the crystallization screening.

Crystallization was performed with hanging-drop methods; equal volumes of protein solution and precipitant were mixed and equilibrated against 0.5 ml precipitant solution. Hampton Research sparse-matrix screens were repeated with inclusion of different transition and heavy-metal ions. Data were collected with a Rigaku (RU-300) X-ray generator and a MAR345 image-plate detector. Data were indexed, processed and reduced using *MOSFLM* (Leslie, 1992) and *SCALA* from the *CCP4* program suite (Collaborative Computational Project, Number 4, 1994). Scaling of data sets, heavy-atom positions and SIR phases were calculated with *CNS* (Brünger *et al.*, 1998).

3. Results and discussion

Although the overall sequence identity of the N-domain of Ca-ATPase and Na,K-

ATPase is low, the domain is flanked by a conserved phosphorylation site on the N-terminal side and a conserved DPP motif on the C-terminal side (not shown). Defining the domain boundaries was therefore straightforward. Fig. 1 shows the corresponding segment in Ca-ATPase together with a sequence alignment.

Expression of the recombinant protein was sufficient for purification and screening of crystallization conditions. The Ni-agarose chromatography fractions showed only a few minor contaminations, which were removed during the subsequent ion-exchange chromatography step. The protein was soluble and could be handled and concentrated as a soluble protein. The yield was about 5–6 mg of purified protein per litre of cell culture, although only the peak fractions with the highest protein concentration from the ion-exchange chromatography were buffer-exchanged and concentrated for crystallization trials.

The protein was crystallized by vapour equilibration against 1.7–2.0 M ammonium sulfate in 50 mM Tris pH 8–9 in the presence of 1 mM NiCl₂. The crystals, shown in Fig. 2, belong to the face-centered cubic space group *F*₂₃, with unit-cell parameters $a = b = c = 147.5 \text{ \AA}$, $\alpha = \beta = \gamma = 90^\circ$. The V_M is $2.8 \text{ \AA}^3 \text{ Da}^{-1}$, corresponding to a solvent content of 56%. Space groups *F*₄₃₂ and *F*_{4,32} could be ruled out since the asymmetric unit would be too small to host the 24 kDa protein; the presence of reflections $h00$ where $h = 2n + 2$ is also incompatible with the *F*_{4,32} screw axis. The crystals could be flash-frozen in the mother liquor with 50% (w/v) sucrose. Native data were

Table 1

Data statistics for native and thimerosal-treated crystals.

The two data sets could be scaled with an *R* factor of 28%. Identification of five mercury sites yielded a phasing power and R_{cullis} of 1.8 and 0.63, respectively. Values in parentheses are for the highest resolution shell.

	Native	Hg derivative
Resolution (Å)	20.0–3.1 (3.27–3.10)	20.0–3.2 (3.37–3.20)
No. of unique reflections	4934 (722)	4523 (683)
Completeness (%)	96.6 (100.0)	99.8 (100)
R_{sym} (%)	8.8 (30.0)	10.1 (38.3)
Multiplicity	7.3 (6.2)	5.7 (4.2)
$I/\sigma(I)$	8.2 (2.6)	6.7 (2.0)

collected to 3.1 Å at 100 K as shown in Table 1.

Initial attempts to solve the structure by molecular replacement using the Ca-ATPase N-domain failed. Addition of 1–2 mM thimerosal directly to the hanging drops resulted in a derivative with five incorporated Hg atoms (Table 1). The *B* factors of the Hg atoms ranged from 4 to 65 Å² after PC refinement with *CNS* (Brünger *et al.*, 1998). A sixth site with a *B* factor of 180 Å² was discarded. Phases derived from isomorphous differences ($R_{\text{scale}} = 0.28$ to 3.2 Å resolution) had a figure of merit of 0.38, which was improved to 0.89 by solvent flipping (Abrahams & Leslie, 1996). Some of the β-strands can be visualized in the electron-density maps calculated from these phases. Fig. 3 shows the electron-density maps calculated from initial and solvent-flipped phases. However, more intense synchrotron radiation will be used in order to collect higher resolution data and obtain better phases.

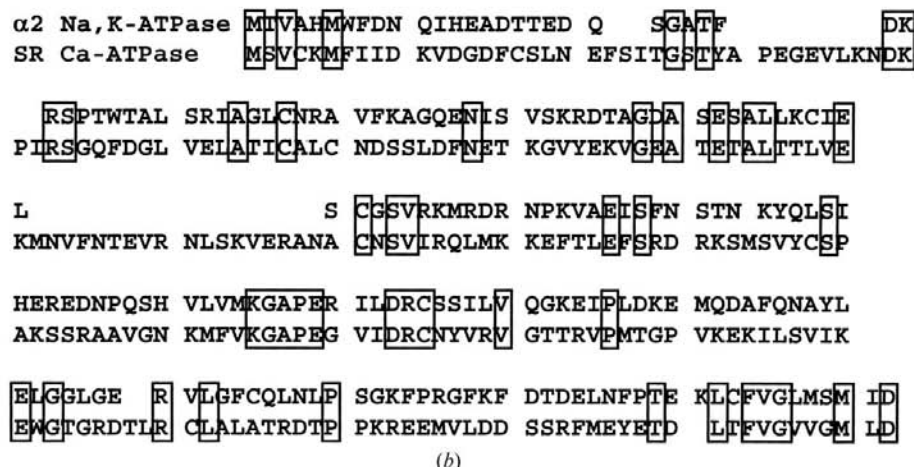


Figure 1

(a) Ca-ATPase structure with the selected N-domain fragment represented by a thick line. (b) Sequence alignment of the cloned α₂ Na,K-ATPase fragment, to which an additional N-terminal methionine and six C-terminal histidines were added, and the homologous segment from Ca-ATPase. The number of identical residues, shown in frames, correspond to 22% of the Na,K-ATPase sequence and 19% of the Ca-ATPase sequence.

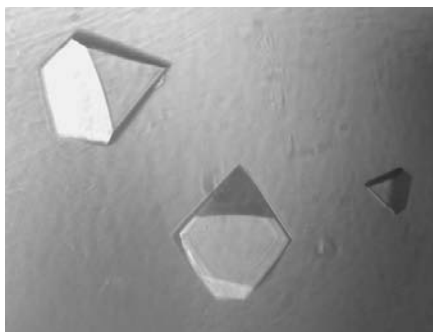


Figure 2
Crystals of the N-domain of porcine α_2 Na,K-ATPase.

The entire cytoplasmic N- and P-domain fragments from rat and mouse Na,K-ATPase have been expressed and purified, and shown to bind ATP (Gatto *et al.*, 1998). We tried a similar approach using porcine Na,K-ATPase, but the expression yield was poor and the product was difficult to obtain in high concentration. The smaller fragment consisting of the N-domain only, when cloned in the same manner into a pQE-40 vector, resulted in better expression and a more soluble specimen suitable for crystallization studies. Of two different isoform N-domains that were cloned and purified, only that of porcine α_2 was crystallized.

Several structures of single-pass transmembrane helix proteins have been elucidated by crystallization of their soluble domains. Pioneering studies of this kind includes the crystallization of influenza virus haemagglutinin after proteolytic release of the external soluble domain (Brand & Skehel, 1972). Such domains can now be expressed and produced through molecular-biology protocols, as exemplified by the recent structures of carbonic anhydrase IV and XII (Stams *et al.*, 1996; Whittington *et al.*, 2001). We show that the technique is not limited to single-span or lipid-anchored

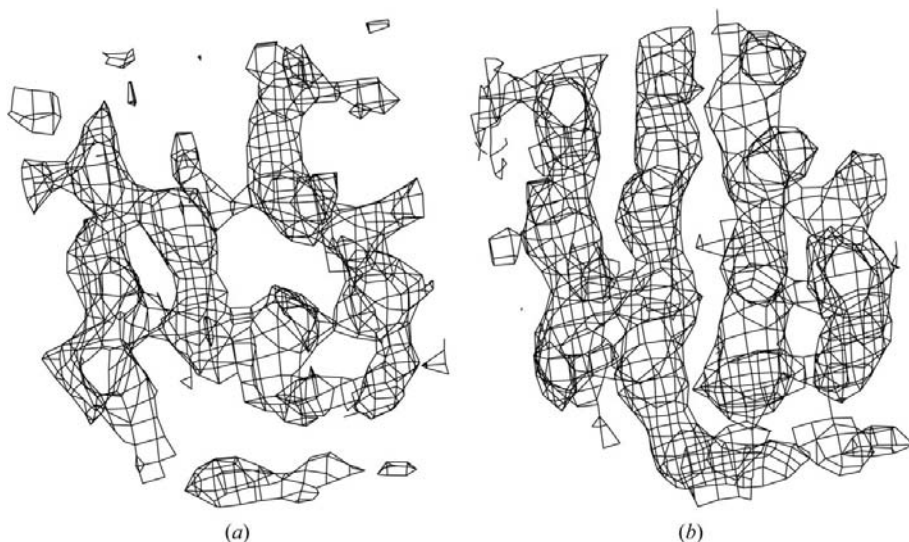


Figure 3
Fourier maps from SIR phasing with a mercury derivative before (a) and after (b) solvent flipping. Both maps show the same section from the same orientation and are contoured at 1σ . The characteristic features of a β -sheet emerge after solvent flipping.

proteins, but can also be applied to internal domains of multispan membrane proteins.

Carina Nielsen and David Sørensen are thanked for technical assistance. We are grateful to Professor Sine Larsen for access to X-ray data-collection facilities and Dr Klavs Hendil for the crystal photograph. This work was supported by the Danish Research Council and the Carlsberg foundation.

References

- Abrahams, J. P. & Leslie, A. G. W. (1996). *Acta Cryst.* **D52**, 30–42.
 Brand, C. M. & Skehel, J. J. (1972). *Nature New Biol.* **238**, 145–147.
 Brünger, A. T., Adams, P. D., Clore, G. M., DeLano, W. L., Gros, P., Grosse-Kunstleve, R. W., Jiang, J. S., Kuszewski, J., Nilges, M., Pannu, N. S., Read, R. J., Rice, L. M., Simonson, T. & Warren, G. L. (1998). *Acta Cryst.* **D54**, 905–921.

- Collaborative Computational Project, Number 4 (1994). *Acta Cryst.* **D50**, 760–763.
 Corpet, F. (1988). *Nucleic Acids Res.* **16**, 10881–10890.
 Deguchi, N., Jorgensen, P. L. & Maunsbach, A. B. (1977). *J. Cell. Biol.* **75**, 619–634.
 Gatto, C., Wang, A. X. & Kaplan, J. H. (1998). *J. Biol. Chem.* **273**, 10578–10585.
 Hebert, H., Purhonen, P., Vorum, Thomsen, H. K. & Maunsbach, A. B. (2001). *J. Mol. Biol.* **314**, 479–494.
 Leslie, A. G. W. (1992). *Jnt CCP4/ESF-EACMB Newsl. Protein Crystallogr.* **26**.
 Skou, J. C. (1957). *Biochim. Biophys. Acta*, **23**, 394–401.
 Stams, T., Nair, S. K., Okuyama, T., Waheed, A., Sly, W. S. & Christianson, D. W. (1996). *Proc. Natl Acad. Sci. USA*, **93**, 13589–13594.
 Toyoshima, C., Nakasako, M., Nomura, H. & Ogawa, H. (2000). *Nature (London)*, **405**, 647–655.
 Toyoshima, C. & Nomura, H. (2002). *Nature (London)*, **418**, 605–611.
 Whittington, D. A., Waheed, A., Ulmasov, B., Shah, G. N., Grubb, J. H., Sly, W. S. & Christianson, D. W. (2001). *Proc. Natl Acad. Sci. USA*, **98**, 9545–9550.